

$1.810 \pm 0.002 \times 10^8 \text{ ms}^{-1}$ ,  $1.87 \pm 0.01 \times 10^8 \text{ ms}^{-1}$ , and  $1.768 \pm 0.002 \times 10^8 \text{ ms}^{-1}$ .

The phase velocity indicates the relative containment of the electromagnetic field within the dielectric. As might be expected, the Earth-neutral configuration, using the outer two conductors of the cable, has a greater proportion of field in air and, hence, the effect of the dielectric in decreasing the velocity is smaller. The unbalanced (Earth and neutral-phase) configuration has the greatest containment of the field and, hence, the effect of the dielectric is largest.

### C. Attenuation Constant

The attenuation constant  $\alpha$  was also found to rise with increasing frequency (see Fig. 4). A first estimate of this loss is the range  $4.3 - 7.7 \times 10^{-9} \text{ dB/Hz/m}$ . Considering the relative containment of the field in the dielectric, we might expect the balanced configurations to exhibit less loss than the unbalanced configurations. However, the increased loss of the balanced configurations appears to be an indication of the radiated energy due to common-mode current, resulting from the lack of perfect balance. It is to be expected that the phase-neutral configuration cannot make a perfectly balanced transmission line because of the asymmetry caused by the presence of a third conductor.

The two-port method using different cable lengths gave similar results for the attenuation constant.

Both the one- and two-port measurements show a much larger loss (dielectric and/or radiated) than calculation based only on the conductivity of the copper. The calculation gives an attenuation at 300 MHz of  $0.01 \text{ Np/m}^{-1}$  ( $0.09 \text{ dBm}^{-1}$ ), compared to the measured value of about  $0.2 \text{ Np/m}^{-1}$  ( $1.8 \text{ dBm}^{-1}$ ).

## VI. CONCLUSIONS

A one- and two-port method for measuring the characteristics of a balanced line, embedded behind some network (balun), were presented and applied to measurements of domestic power cabling. Though this application used submicrowave frequencies, the techniques are applicable to higher (including microwave) frequencies. The two-port method only gives the propagation constant, but is superior for attenuation measurements.

To obtain repeatable measurements, a good balun is necessary. This is because any common-mode current component is prone to radiate. It was found that a fine coax wound on a high-permeability toroid made a suitable balun.

The three conductor line under test was connected in three different connection configurations. The characteristic impedance was found to be almost purely resistive, and varies very little with frequency. The phase constant increases almost linearly with frequency, indicating a constant phase velocity. The phase velocity is lower for the configurations having a higher proportion of the electromagnetic field contained within the cable insulation, as expected. The attenuation also shows an increase with frequency, although with a much greater fluctuation. Most of this loss appears to be caused by the cable insulation, with a small component of copper loss, and some radiation caused by imperfection in the transmission balance.

## REFERENCES

- [1] K. Yanagaw and J. Cross, "Modal decomposition (non-balun) measurement technique: Error analysis and application to UTP/STP characterization to 500 MHz," in *Proc. 44th Int. Wire Cable Symp. (IWCS)*, Philadelphia, PA, Nov. 1995, pp. 126-133.
- [2] D. K. Cheng, *Field and Wave Electromagnetics*. Reading, MA: Addison-Wesley, 1983, pp. 381-382, 386-387.
- [3] R. F. Bauer and P. Penfield Jr., "De-embedding and unterminating," *IEEE Trans. Microwave Theory Tech.*, vol. MTT-22, pp. 283-288, Mar. 1974.
- [4] P. I. Somlo and J. D. Hunter, *Microwave Impedance Measurements*. Stevenage, U.K.: Peregrinus, 1985, p. 6.
- [5] R. B. Marks, "A multiline method of network analyzer calibration," *IEEE Trans. Microwave Theory Tech.*, vol. 39, pp. 1205-1215, July 1991.
- [6] D. A. McClure, "Broadband transmission line transformer family matches a wide range of impedances," *RF Design*, pp. 62-66, Feb. 1994.
- [7] —, "Broadband transmission line transformer family matches a wide range of impedances," *RF Design*, pp. 40-49, May 1995.
- [8] J. Sevick, *Transmission Line Transformers*, 2nd ed. Newington, CT: Amer. Radio Relay League, 1990, pp. 3-15.

## Crossed Dipoles Fed with a Turnstile Network

Robert K. Zimmerman, Jr.

**Abstract**—A "turnstile network" is introduced which may be conveniently used for circular polarization synthesis. The network, outfitted with proper phasing stubs, forms a balanced quadrature hybrid; for an antenna with less than a perfect reflection coefficient, the reflected power will appear at an isolated port, which may be terminated, resulting in good polarization properties coupled with good input voltage standing-wave ratio. A crossed-dipole array is used as a test-bed to demonstrate the turnstile network.

**Index Terms**—Antenna components, antenna feeds, circular polarization.

## I. INTRODUCTION

Dicke invented the waveguide turnstile during World War II at the Massachusetts Institute of Technology (MIT) Radiation Laboratory, Cambridge [1]-[3]. The device was patented [4] in 1954 as a network for exciting circularly polarized waves in circular waveguide. Turnstile theory is discussed in some detail in [5].

Presented here is a simple coaxial network which provides the same turnstile function, *but not in waveguide*. Where Dicke's turnstile used reflective waveguide stubs for polarization synthesis, this network uses reflective coaxial stubs.

## II. PROPOSED NETWORK AND FEED

Fig. 1 shows the proposed network and feed. The feed is a crossed-dipole array residing within a cavity. The turnstile network comprises four coaxial transmission-line segments, each  $\lambda/4$  in length at center frequency, and which, for this discussion, are assumed to have a  $50\Omega$  characteristic impedance. The four segments of transmission line form a star network: all four shields are connected together and all four inner conductors are joined at the bottom of the network. The network has fourfold rotational symmetry, as required by theory [1].

Manuscript received December 3, 1997; revised August 1, 1998.

The author was with the Arecibo Observatory, Arecibo, PR 00614 USA. He is now with the Los Alamos National Laboratory, LANSCE 5, MS H827, Los Alamos, NM 87545 USA.

Publisher Item Identifier S 0018-9480(98)09058-9.

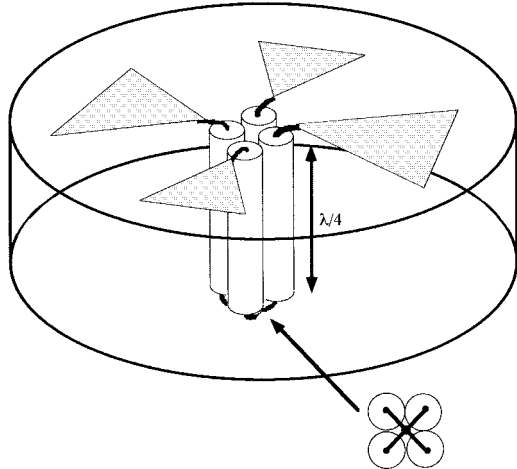


Fig. 1. Possible layout of a turnstile network connected to a crossed-dipole array within a cavity reflector. This layout was not used.

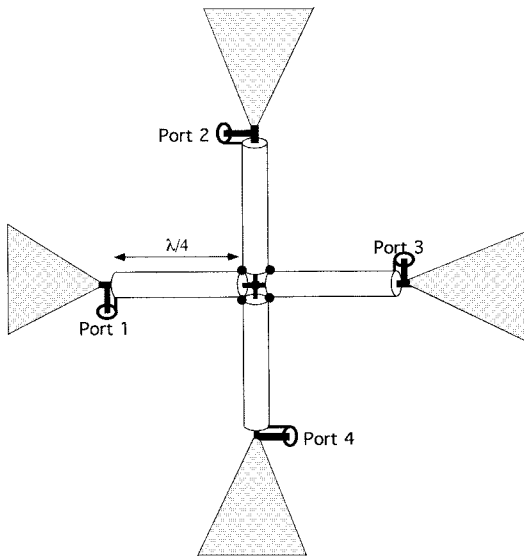


Fig. 2. Exploded view of turnstile network and antenna elements showing the four ports.

For purposes of concept explaining, Fig. 1 does not show the ports. The four ports are shown in the exploded view in Fig. 2, labeled 1–4. A short, but complete, analysis (at center frequency) may be made by considering the following odd and even cases.

#### A. Odd Case

Suppose two opposite ports are driven at center frequency “out-of-phase.” The remaining two ports are terminated. The case is shown in Fig. 3(a). No current passes down the transmission line between opposite ports because it is  $\lambda/2$  in length (overall) at the driven frequency. Ports 1 and 3 will be totally matched if the dipole has a differential drive impedance of  $100 \Omega$ , which would yield  $50 \Omega$  at port 1 and  $50 \Omega$  at port 3. There is no voltage at the center connection of the star. Consequently, no voltage is transmitted to ports 2 or 4. Loads at ports 2 and 4 are isolated.

#### B. Even Case

Suppose ports 1 and 3 are now driven at center frequency “in-phase.” This case is shown in Fig. 3(b). Power will flow from

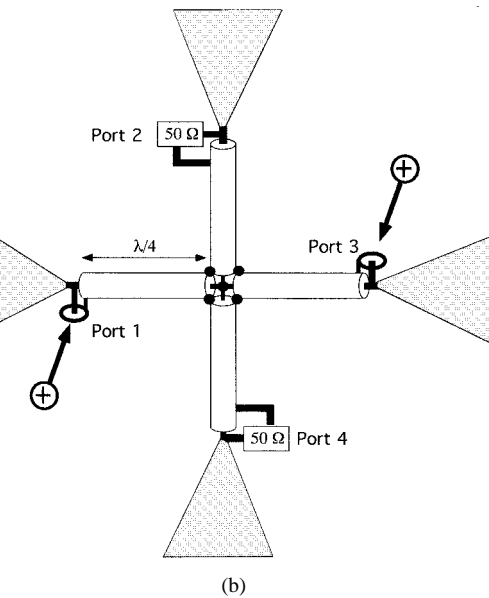
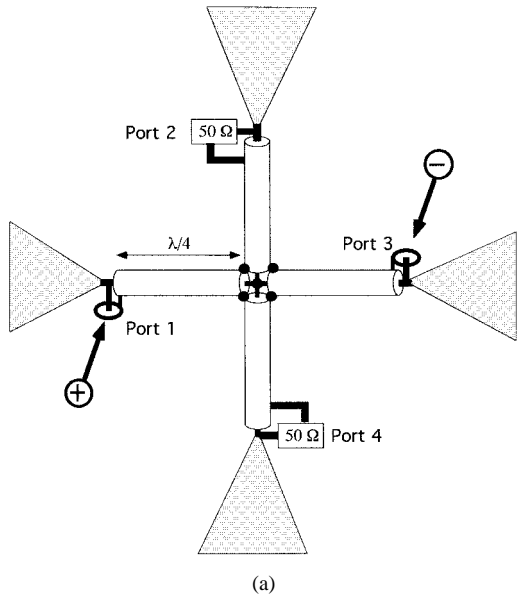


Fig. 3. (a) Turnstile network (and antenna elements) arranged so that ports 1 and 3 are driven out-of-phase. Ports 2 and 4 are isolated. (b) Turnstile network (and antenna elements) arranged so that ports 1 and 3 are driven in-phase. Ports 2 and 4 are terminated in  $50 \Omega$ .

ports 1 and 3 through the star network to ports 2 and 4. The dipole arms (in the cavity) will result in some reactive loading of the network since adjacent arms are  $180^\circ$  apart in phase. However, if the dipoles are well within the cavity, there will be no radiation loss. The reactive loading of the dipole arms may be canceled by placing a reactance (of the same sign) at the center node of the star network ( $\lambda/4$  from each port). This reactance may be adjusted until all the power entering ports 1 and 3 flows to the loads at ports 2 and 4. (Keep in mind that this reactance can in no way affect the “odd” mode discussed earlier since there is no voltage at the center of the network for that mode.)

We have now seen that the odd and even cases may be perfectly matched ( $50 \Omega$ ) if the dipole impedance is  $100 \Omega$  and a nulling reactance is placed in the network at the central node. With these conditions, we may use superposition to show that any (coherent) input to ports 1 and 3 will also be matched. For example, consider

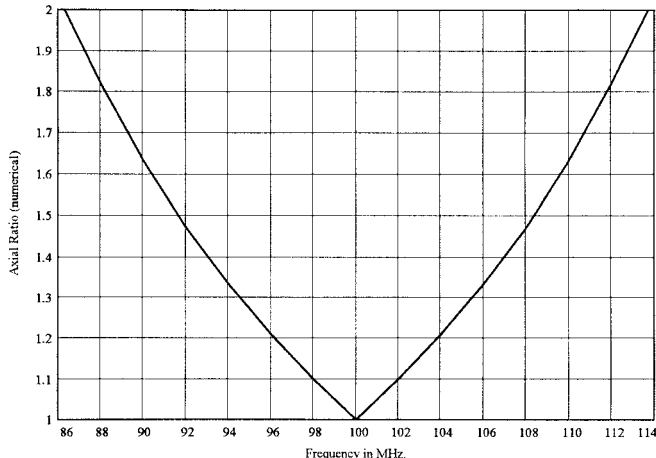


Fig. 4. Axial ratio versus frequency. Modeled axial ratio from a crossed-dipole array fed with a turnstile network (with  $45^\circ$  open and shorted phasing stubs so as to act as a polarizer).

an input to port 1 alone. Using vector notation, an input to port 1 may be represented as the following superposition:

$$\begin{bmatrix} 1 \\ 0 \\ 0 \\ 0 \end{bmatrix} = \begin{bmatrix} \frac{1}{2} \\ 0 \\ -\frac{1}{2} \\ 0 \end{bmatrix}_{\text{Odd}} + \begin{bmatrix} \frac{1}{2} \\ 0 \\ \frac{1}{2} \\ 0 \end{bmatrix}_{\text{Even}}.$$

It follows immediately that port 1 is matched. For the port-1 drive, the “odd” portion of the drive will be radiated (1/2 power), while the “even” portion of the drive will be absorbed by loads two and four (1/4 power each).

### III. POLARIZATION SYNTHESIS

Now consider port 1 being driven in the following context. Suppose that the loads are removed from ports 2 and 4, and instead we attach a  $45^\circ$   $50\Omega$  *shorted* cable to port 2 and a  $45^\circ$   $50\Omega$  *open* cable to port 4. The voltage at port 2 will be reflected from its phasing stub at an angle of  $270^\circ$ . The voltage at port 4 will be reflected from its phasing stub at  $90^\circ$ . Accordingly, ports 2 and 4 (originally “in-phase”) are now driven “out-of-phase” and *in quadrature* with port 1. Circular polarization will result: port 1 will be one polarization and port 3 will be the orthogonal polarization. Or, if the network is thought of as a quadrature hybrid, port 1 will be the input port, while port 3 is the isolated port.

Note that it is not necessary to use an open stub for polarization synthesis—it is only necessary that the reflected phases at ports 2 and 4 be  $180^\circ$  apart. Accordingly, for high-power work, it might be desirable to use two properly cut shorted stubs.

### IV. MODELING

An EESoF Touchstone model of a turnstile network was checked to examine the potential bandwidth of the network as a circular polarizer. Ports 2 and 4 were connected to open and shorted lines  $45^\circ$  long at center frequency (100 MHz). The dipole arms were replaced with coupling transformers, yielding two “circular” coaxial output channels. An axial ratio of 1.5:1 was achieved over a 16% bandwidth. The actual plot is presented in Fig. 4.

Using the turnstile network to improve the voltage standing-wave ratio (VSWR) of an antenna is easy to analyze. From [5], the input reflection coefficient for drive to port 1 is

$$S_{11} = (\Gamma_{\text{even}} + \Gamma_{\text{odd}})/2$$

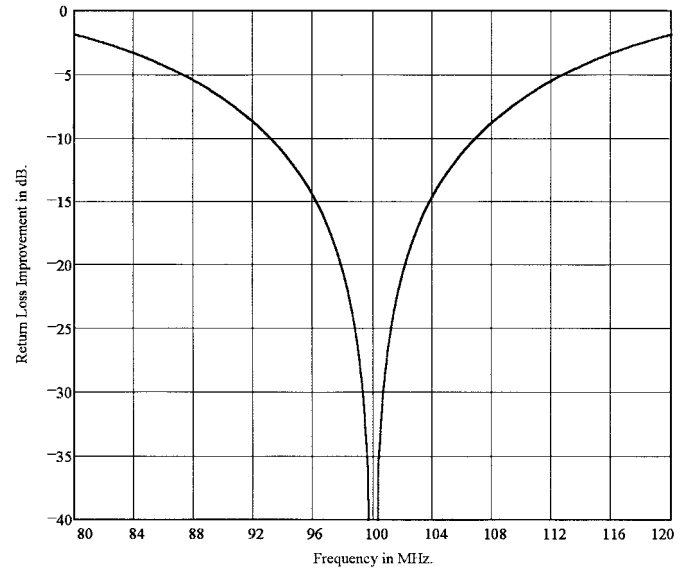


Fig. 5. Return-loss improvement provided by the turnstile network. This is a plot of the input return-loss improvement that can be accomplished over  $\Gamma_{\text{odd}}$  alone by using the network as a hybrid (where  $\Gamma_{\text{odd}}$  and  $\Gamma_{\text{even}}$  effectively cancel).

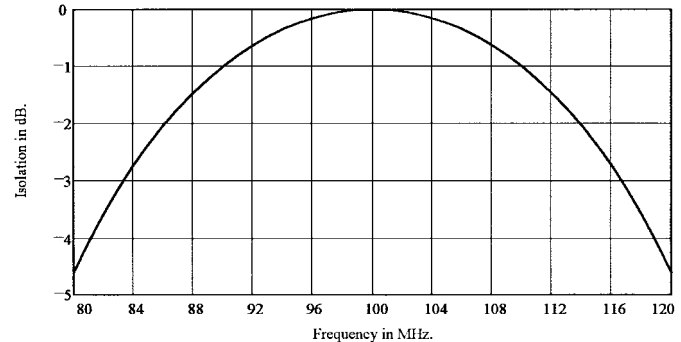


Fig. 6. Turnstile network isolation (ports 1 to 3) measured with respect to  $\Gamma_{\text{odd}}$  alone. Note that at center frequency, where the turnstile acts as a perfect hybrid,  $\Gamma_{\text{odd}}$  maps right through the network (as it must).

where  $\Gamma_{\text{even}}$  and  $\Gamma_{\text{odd}}$  are the reflection coefficients for the symmetric and antisymmetric drive cases presented earlier. (These special reflection coefficients may be measured using in-phase and out-of-phase power splitters with a network analyzer.) Consider the odd case first, for which there is never any voltage at the center node of the network. Accordingly, we can short the center node and immediately express the impedance at ports 1 and 3 as the parallel combination of a dipole arm in parallel with a quarter-wave shorted stub

$$Z_{\text{odd}} = [Z_{\text{dipole arm}}][jZ_0 \tan(2\pi L_o/\lambda)]/[Z_{\text{dipole arm}} + jZ_0 \tan(2\pi L_o/\lambda)]$$

where  $L_o$  is the length of the four “star” transmission lines. Therefore,

$$\Gamma_{\text{odd}} = (Z_{\text{odd}} - 50)/(Z_{\text{odd}} + 50).$$

The even case is simple as well. With ports 1 and 3 driven in-phase, the applied excitation first travels through the network to ports 2 and 4, undergoing a phase delay of  $-(2L_o/\lambda)2\pi$ . The signals then travel down the phasing cables, returning to ports 2 and 4 exactly out-of-phase (assuming the cables are “open” and “short”). The signal which reflected off the open cable, experienced a phase shift of  $-(2L_1/\lambda)2\pi$ , where  $L_1$  is the length of the phasing stub.

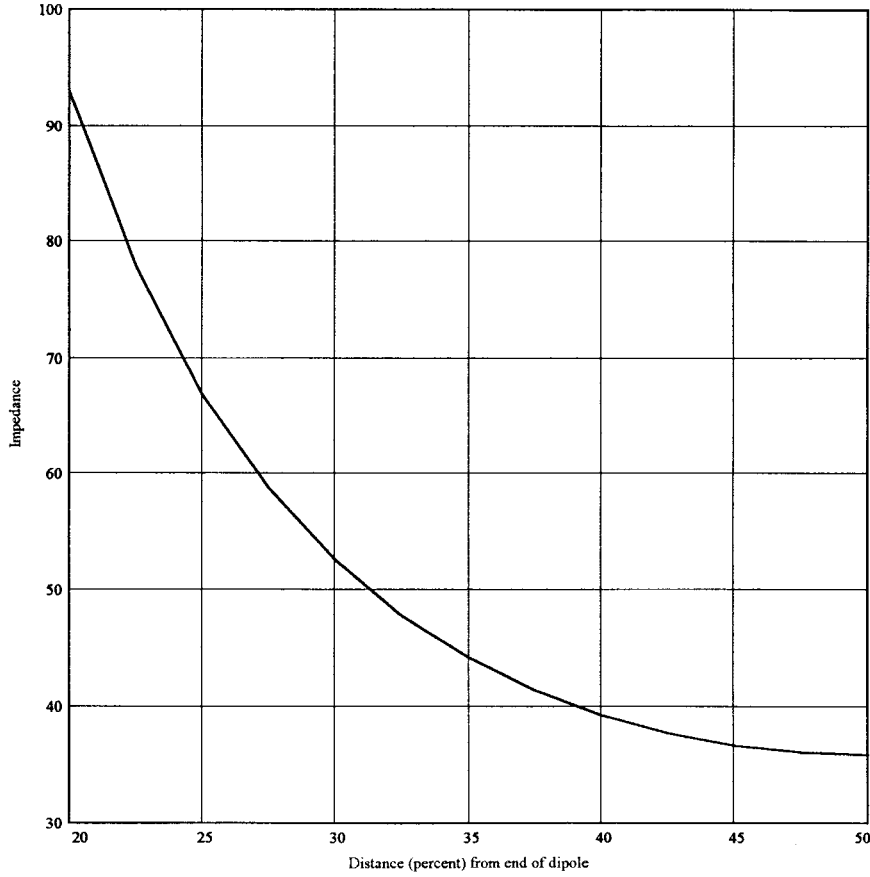


Fig. 7. Real( $Z$ ) versus feed location. Dipole antenna resonant impedance (real) as a function of the location of dual symmetric feed points. As the feed points are moved out toward the ends of the dipole, the impedance rises as shown.

These out-of-phase signals (at ports 2 and 4) then experience a reflection  $\Gamma_{\text{odd}}$ . There is then another trip down and up the phasing stubs, and finally, the trip back through the network to ports 1 and 3. The entire even reflection coefficient is then

$$\begin{aligned}\Gamma_{\text{even}} &= \exp(-j4\pi L_0/\lambda) \exp(-j4\pi L_1/\lambda) \\ &\quad \cdot \Gamma_{\text{odd}} \exp(-j4\pi L_1/\lambda) \exp(-j4\pi L_0/\lambda) \\ &= \Gamma_{\text{odd}} \exp[-j8\pi(L_0 + L_1)/\lambda].\end{aligned}$$

Accordingly, the total reflection coefficient for the port-1 drive is

$$S_{11} = \Gamma_{\text{odd}}[1 + \exp(-j8\pi(L_0 + L_1)/\lambda)]/2.$$

The factor multiplying  $\Gamma_{\text{odd}}$  is plotted in Fig. 5, showing the improvement which can be obtained in the input return loss by using the turnstile as a hybrid. The curve was verified with an EESoF model.

When port 1 is driven and port 3 is terminated, power backscattered into the turnstile network from the antenna will tend to appear at the port-3 termination. From [5], the incurred isolation is

$$S_{31} = (\Gamma_{\text{even}} - \Gamma_{\text{odd}})/2$$

which we may now write as

$$S_{31} = \Gamma_{\text{odd}}[-1 + \exp(-j8\pi(L_0 + L_1)/\lambda)]/2.$$

The factor multiplying  $\Gamma_{\text{odd}}$  is plotted in Fig. 6, showing how the opposite port isolation will vary over frequency. Note that at center

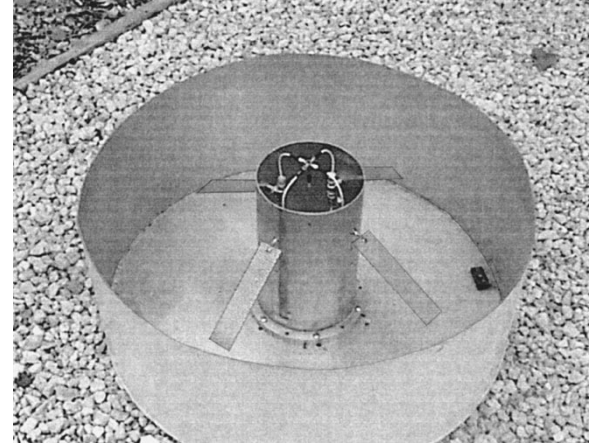


Fig. 8. Photograph of 350-MHz crossed-dipole cavity feed. The turnstile network is contained within the central cylinder. The dipole arms were bent down experimentally to obtain a good match when fed with an out-of-phase power splitter.

frequency (where the network functions as a perfect hybrid),  $\Gamma_{\text{odd}}$  maps right through, as it must.

Before building a prototype antenna, the author had intended to use dipoles, as depicted in Fig. 1. However, the feed-point impedance of a dipole fed at the center is  $73 \Omega$ . For dual feed points (equally spaced from the center of the dipole) the drive impedance increases as the feed points are moved further out along the dipole. This effect is shown in Fig. 7, taken from an ELNEC model. Thus, dual

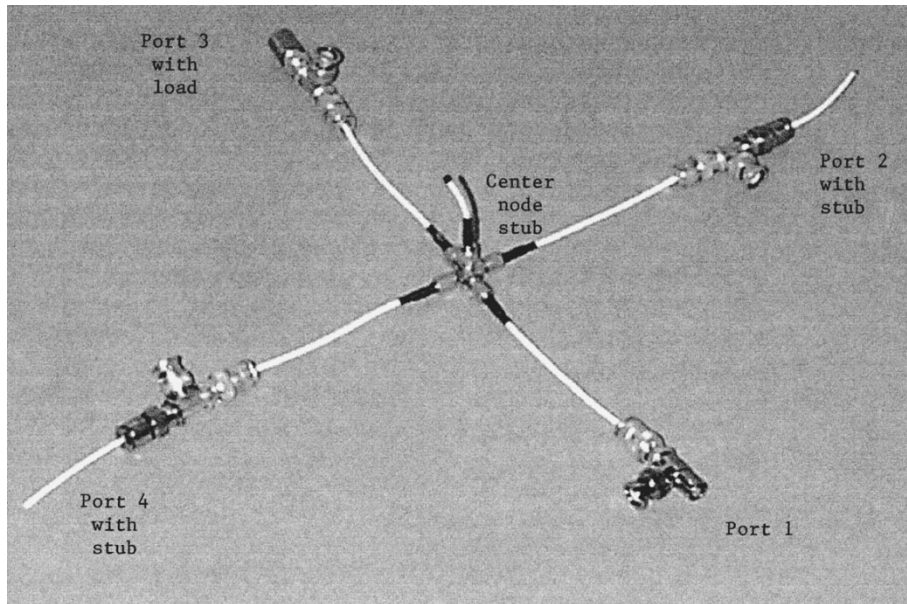


Fig. 9. Close-up photo of the turnstile network. At the central node is a shorted stub for reactance nulling when the network is driven in even mode. The two stubs for circular polarization can be seen at ports 2 and 4. Port 1 is for a single-cable drive, while port 3 is terminated.

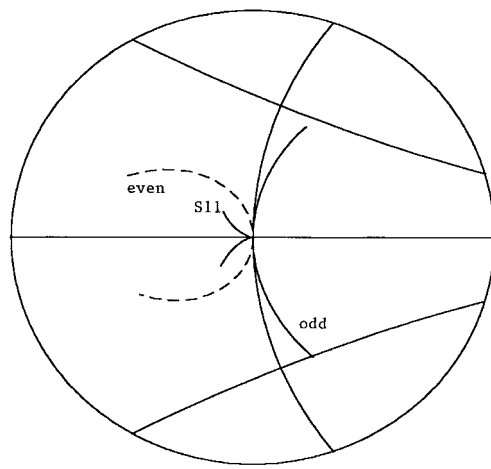


Fig. 10. Composite data plot showing  $\Gamma_{\text{even}}$ ,  $\Gamma_{\text{odd}}$ , and  $S_{11} = (\Gamma_{\text{odd}} + \Gamma_{\text{even}})/2$  with the circular phasing stubs installed at ports 2 and 4. The outer radius is  $\Gamma_{\text{max}} = .333$ .

50- $\Omega$  drives can be achieved when the drive points are symmetrically spaced about 32% from each dipole end.

## V. PROTOTYPE

A 350-MHz prototype was built in a 75-cm-diameter cavity, as depicted in Fig. 8. The turnstile network is contained within the 17.8-cm-diameter support cylinder. Fig. 9 shows the turnstile network removed from the feed. The prototype dimensions may be scaled for other frequencies. Fig. 10 is a composite data plot showing  $\Gamma_{\text{odd}}$ ,  $\Gamma_{\text{even}}$ , and  $S_{11} = (\Gamma_{\text{odd}} + \Gamma_{\text{even}})/2$  with the circular phasing stubs installed at ports 2 and 4. The feed was pointing toward free space.  $\Gamma_{\text{odd}}$  was measured with a Mini-Circuits ZFSCJ-2-4 180° power splitter connected to ports 1 and 3.  $\Gamma_{\text{even}}$  was measured with a Mini-Circuits ZFSC-2-4 0° power splitter connected to ports 1 and 3. The center node reactance used for nulling  $\Gamma_{\text{even}}$  was a shorted coaxial stub providing  $+10j \Omega$  at 350 MHz.  $S_{11}$  was measured driving port 1 directly with a termination installed at port 3. Fig. 11 is the same data

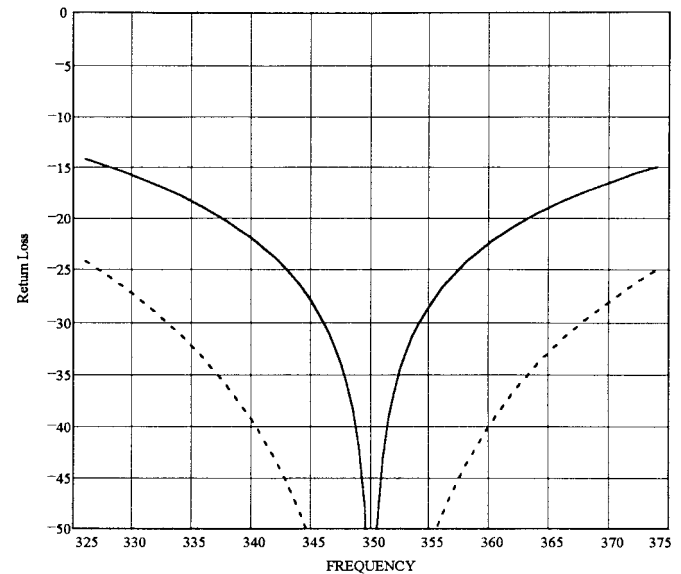


Fig. 11. Return loss plot showing the same data as in Fig. 10. The upper trace represents  $\Gamma_{\text{odd}}$  and  $\Gamma_{\text{even}}$ . The lower plot shows the return-loss improvement using the turnstile network as a quadrature hybrid.

set displayed in a return loss plot. ( $\Gamma_{\text{odd}}$  and  $\Gamma_{\text{even}}$  have the same trace.)

The axial ratio was not measured, but is believed to be well represented by Fig. 5.

## VI. SUMMARY

A new network, which we call a “turnstile network,” has been proposed and investigated for feeding crossed dipoles in a manner convenient for circular polarization synthesis. The network takes the place of two baluns and a quadrature hybrid network. The network allows the arms of a dipole to be spread some distance apart, so as to permit a mechanically robust realization. A simple “even/odd” analysis was used to show that the network is matched for a single input drive. A complete model, developed from simple transmission-

line theory, predicts the return-loss improvement obtained by using the network with a reflective antenna. The network is placed in the context of previous work by Dicke.

#### ACKNOWLEDGMENT

The author is indebted to the National Astronomy & Ionosphere Center (NAIC), Arecibo Observatory, Arecibo, PR, for time and facilities to develop the turnstile network. Cornell University operates NAIC under a cooperative agreement with the National Science Foundation.

#### REFERENCES

- [1] C. G. Montgomery, R. H. Dicke, and E. M. Purcell, "Principles of microwave circuits," *Radiation Lab. Series*, vol. 8, pp. 459-466, 1948.
- [2] G. L. Ragan, "Microwave transmission circuits," *Radiation Lab. Series*, vol. 9, pp. 375-377, 1948.
- [3] M. A. Meyer and H. B. Goldberg, "Applications of the turnstile junction," *IRE Trans. Microwave Theory Tech.*, vol. MTT-3, pp. 40-45, Dec. 1955.
- [4] R. H. Dicke, "Turnstile junction for producing circularly polarized waves," U.S. Patent 2 686 901, Aug. 17, 1954.
- [5] R. K. Zimmerman, Jr., "Resonant disk turnstile," *IEEE Trans. Microwave Theory Tech.*, vol. 45, pp. 1600-1610, Sept. 1997.

## A Simple Method for Blocking Parasitic Modes in a Waveguide-Packaged Microstrip-Line Circuit

Hao-Hui Chen, Chun-Long Wang, and Shyh-Jong Chung

**Abstract**—A simple structure formed by two metal patches symmetrically deposited at the two sides of the center microstrip is proposed and analyzed for blocking the higher order modes in a waveguide-packaged microstrip-line circuit. The variations (with the patch width) of the effective dielectric constants and field distributions of the modes in the packaged microstrip line with infinitely long side patches were first investigated using the two-dimensional (2-D) finite-element method (FEM) and the method of lines. The results suggested that there exists a range of patch widths at which the field distributions of the higher order modes are totally different from those of the microstrip line without side patches. The scattering of the patches as a function of the patch length and width was then studied using the three-dimensional (3-D) FEM with edge elements. It has been found that by simply choosing appropriate patch sizes, the parasitic higher order mode can be reflected without sacrificing the normal propagation of the dominant mode.

**Index Terms**—Finite-element method, packaged microstrip line, side patches, spurious modes.

## I. INTRODUCTION

Microwave and millimeter-wave circuits are usually shielded by a rectangular waveguide to prevent the circuits from mechanical destructions and electromagnetic interferences (EMI's) from the

Manuscript received June 25, 1997; revised July 14, 1998. This work was supported by the National Science Council of the R.O.C. under Grant NSC 85-2213-E-009-001.

The authors are with the Department of Communication Engineering, National Chiao Tung University, Hsinchu 30039, Taiwan, R.O.C. (e-mail: sjchnug@cm.nctu.edu.tw).

Publisher Item Identifier S 0018-9480(98)09034-6.

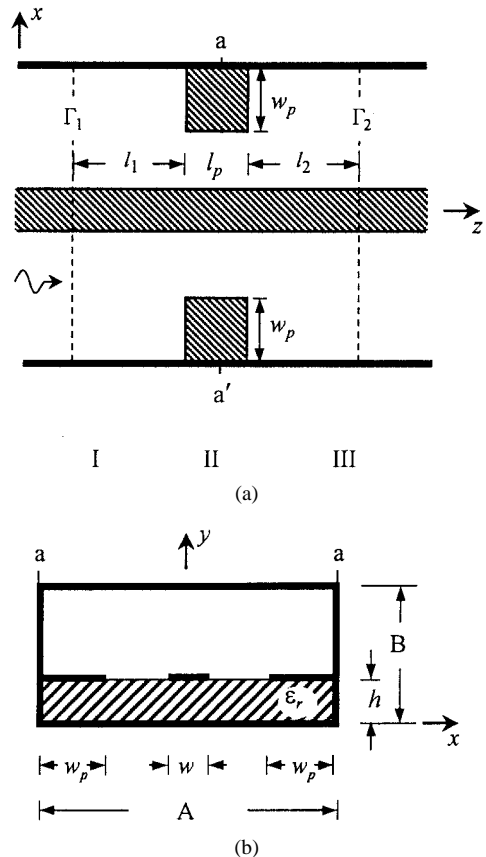


Fig. 1. A waveguide-packaged microstrip line with metal patches deposited at the two sides of the center microstrip.

environment. As the level of the integration and/or the operation frequency increases, parasitic fields may be excited by active devices and/or discontinuities in the circuits and propagate in the form of the higher order modes of the shielded transmission line. When the signals (which are carried by the dominant mode) and the parasitic propagation modes travel from one circuit element toward another one, the power coupling between modes would be caused through the latter circuit element and, thus, disturbs the total circuit operation.

To relieve the circuit element from the EMI caused by the parasitic modes, several possible approaches can be found in [1]–[5]. Deforming the enclosures or using anisotropic substrates can increase the cutoff frequencies of the higher order modes in a packaged microstrip line or a coplanar waveguide [1], [2]. Placing attenuating elements (such as resistive films and microwave absorbers) at appropriate locations can damp the parasitic fields and package resonances [3], [4]. Also, attaching metal diaphragms can reflect the incident higher order modes [5]. Although these designs would reduce the influences of the parasitic waves on the circuit, the constructions of the structures still seemed complicated.

In this paper, we propose a simple design for blocking the higher order modes in a packaged microstrip line. As shown in Fig. 1, this method uses two side metal patches to reflect the incident parasitic modes. The patches are to be etched on the substrate at the same time as the fabrication of the microstrip-line circuit, thus making the design easily realized. In the patch-deposited microstrip-line region, since the dominant mode has most of its field concentrated in the